Clinical Neurophysiology 132 (2021) 1089–1104

Contents lists available at ScienceDirect

Clinical Neurophysiology

journal homepage: www.elsevier.com/locate/clinph

Near-fiber electromyography

Mathew Piasecki [a,*], Oscar Garnés-Camarena [b], Daniel W. Stashuk [c]

[a] Clinical, Metabolic and Molecular Physiology, MRC-Versus Arthritis Centre for Musculoskeletal Ageing Research, National Institute for Health Research (NIHR) Nottingham Biomedical Research Centre, University of Nottingham, Nottingham, United Kingdom
[b] Department of Physical Medicine and Rehabilitation - Clinical Neurophysiology, Jiménez Díaz Foundation University Hospital, Madrid, Spain
[c] Department of Systems Design Engineering, University of Waterloo, Ontario, Canada

ARTICLE INFO

Article history:
Accepted 5 February 2021
Available online 10 March 2021

Keywords:
Near fiber electromyography
Near fiber motor unit potential
Quantitative electromyography

HIGHLIGHTS

- Near fiber EMG (NFEMG) focuses on contributions from individual or small groups of near motor unit fibers to detected near fiber motor unit potentials (MUPs).
- Near fiber MUP duration and dispersion increases can indicate early and progressive axonal sprouting with conduction slowing or neuromuscular junction transmission delay and/or increased MU fiber diameter variability.
- Increases in near fiber MUP jiggle and segment jitter can indicate early and progressive increases in electrophysiological temporal variability for the near fibres (i.e. NF jitter).

ABSTRACT

Objective: Describe and evaluate the concepts of near fiber electromyography (NFEMG), the features used, including near fiber motor unit potential (NFMUP) duration and dispersion, which relate to motor unit distal axonal branch and muscle fiber conduction time dispersion, and NFMUP segment jitter, a new measure of the temporal variability of neuromuscular junction transmission (NMJ), and axonal branch and muscle fibre conduction for the near fibres (i.e. NF jitter), and the methods for obtaining their values.
Methods: Trains of high-pass filtered motor unit potentials (MUPs) (i.e. NFMUP trains) were extracted from needle-detected EMG signals to assess changes in motor unit (MU) morphology and electrophysiology caused by neuromuscular disorders or ageing. Evaluations using simulated needle-detected EMG data were completed and example human data are presented.
Results: NFEMG feature values can be used to detect axonal sprouting, conduction slowing and NMJ transmission delay as well as changes in MU fiber diameter variability, and NF jitter. These changes can be detected prior to alterations of MU size or numbers.
Conclusions: The evaluations clearly demonstrate and the example data support that NFMUP duration and dispersion reflect MU distal axonal branching, conduction slowing and NMJ transmission delay and/or MU fiber diameter variability and that NFMUP jiggle and segment jitter reflect NF jitter.
Significance: NFEMG can detect early changes in MU morphology and/or electrophysiology and has the potential to augment clinical diagnosis and tracking of neuromuscular disorders.

1. Introduction

A motor unit (MU) is comprised of a somatic motor neuron, its axon and distal axonal branches, neuromuscular junctions (NMJs) and associated skeletal muscle fibers. Neuromuscular disorders can affect somatic motor neurons, their axons, axonal branches, NMJs and/or associated muscle fibers. Anatomically neuromuscular disorders can cause loss of somatic motor neurons, axonal demyelination, and MU remodelling; fiber denervation and the

Abbreviations: MU, motor unit; NMJ, neuromuscular junction; MFP, muscle fiber potential; MUP, motor unit potential; EMG, electromyographic; NF, near fiber; NFMUP, near fiber motor unit potential; NFEMG, near fiber electromyography.

* Corresponding author.
E-mail address: mathew.piasecki@nottingham.ac.uk (M. Piasecki).

https://doi.org/10.1016/j.clinph.2021.02.008
1388-2457/

sprouting of new axonal branches and the formation of new NMJs, acting to minimise muscle fiber loss; and fiber atrophy and/or hypertrophy (Piasecki et al., 2016b). Electrophysiologically, neuromuscular disorders can cause axonal conduction slowing, NMJ transmission delay, muscle fibre conduction variability, increased NMJ transmission time variability and/or NMJ transmission failure (Daube, 2000).

The discharge/activation of a motor neuron creates a transaxolemmal action potential, which propagates along its axon and each axonal branch to initiate NMJ transmission to its associated muscle fiber. The consequent generation of propagating transsarcolemmal or muscle fibre action potentials (MFAPs) results in coordinated muscle contraction. As such, the MU is the fundamental element of muscle force generation (Heckman and Enoka, 2012). As depicted in Fig. 1, extracellularly recorded motor unit potentials (MUPs) are comprised of the summation of muscle fibre potentials (MFPs) generated by propagating MFAPs. During muscle activation, populations of MUs are recruited and discharge at pseudo-regular firing times, with each MU generating a set of consecutively generated MUPs or a MUP train. As such, EMG signals are comprised of temporally overlapped sets of MUP trains and can be used to estimate the extent of anatomical and electrophysiological alterations.

With simple level or window triggering or more sophisticated pattern recognition methods, MUP trains can be extracted from a recorded EMG signal. The number of trains extracted can be indicative of the level of MU recruitment. MUP occurrence times within a MUP train directly relate to the discharge pattern of its corresponding MU. MU recruitment and discharge patterns are both related to a combination of muscle anatomy and electrophysiology. For known levels of activation, the number of motor neurons recruited, their discharge patterns and anatomical characteristics can be used to infer the presence and extent of a neuromuscular disorder (Sonoo, 2002). A MUP template, either a representative MUP selected from the MUPs within the train or a waveform calculated using the MUPs of the train, can be used to infer MU anatomical features, such as size and the extent of distal axonal branching. MUP shape instability within a train can be used to infer electrophysiological features, such as the temporal variability of NMJ transmission, and axonal branch and muscle fiber conduction for the MU fibres near to the recording electrode (i.e. near fibre jitter). NMJ transmission time variability is related to the dynamics of acetylcholine release and binding of across the NMJ. While axonal branch and muscle fibre conduction time variability is related to variations in action potential conduction velocity along the axolemmal and sarcolemma of axonal branches and muscle fibres, respectively. However, because NMJ transmission time variability is often much greater than axonal branch and muscle fiber conduction time variability (Katz and Miledi, 1965; Siegelbaum and Koester, 2013) greater MUP shape instability often reflects mostly NMJ transmission time variability.

More specifically, standard clinical EMG examinations are now based on signals detected using concentric or monopolar needle electrodes. Initially, with the muscle at rest, spontaneous activity is qualitatively or semi-quantitatively assessed for signs of denervation. Then during low levels of activation, MUP trains are extracted and a MUP template is obtained. Increased or decreased MUP template duration, amplitude and/or area can be indicative of MU re-innervation or fiber loss, atrophy or NMJ blocking, respectively. The number of MUP template phases and/or turns can be indicative of MU axonal sprouting and/or fiber atrophy or hypertrophy. During varying levels of activation, MU recruitment and discharge patterns are qualitatively or semi-quantitatively assessed.

Specific aspects of neuromuscular disease could be better detected if signals better reflecting the anatomical and electrophysiological effects of disease on individual muscle fibers could be assessed. In general, it is not possible to detect only the MFP from a single muscle fiber. However, as the characteristics of an MFP generated by a muscle fiber are dependent on fiber diameter and its radial distance to the electrode detection surface, as radial distance increases, the amplitude and high frequency content of a detected MFP decreases. This means that MFP contributions to a MUP from distant fibers will be of lower amplitude and have a

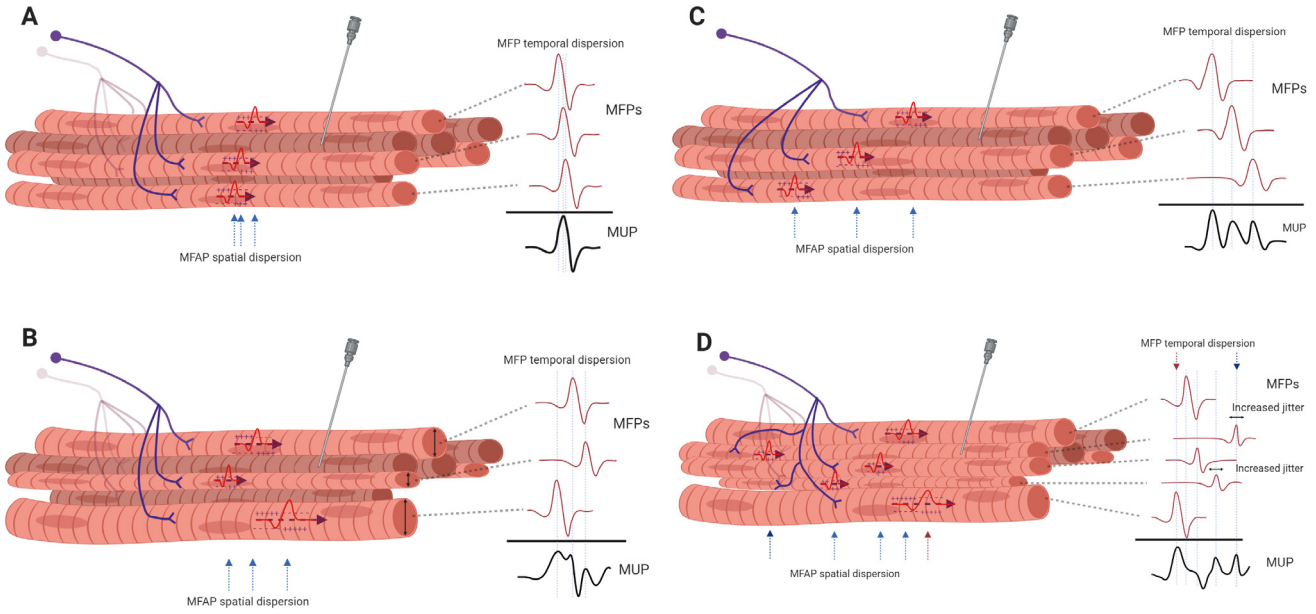

Fig. 1. Schematic of MU activation and external MUP detection, four scenarios are depicted: healthy 1A; increased fibre diameter variability 1B; increased endplate scatter 1C; and reinnervation 1D. For each scenario, propagating MFAPs at a specific point in time as well as the extent of MFAP spatial dispersion are depicted on the left and the corresponding MFPs, their MFP temporal dispersion and the ensemble summed MUP are depicted on the right. All depictions are conceptual and not to scale. In 1D, increased MFP jitter for the newly reinnervated fibres is indicated by arrows placed across the lines demarcating the corresponding MFP peak locations. MFAP, muscle fiber action potential; MFP, muscle fiber potential; MUP, motor unit potential.

greater proportion of lower frequency energy. Conversely, MFP contributions from near fibers (NFs) will be of higher amplitude and have a greater proportion of higher frequency energy. As suggested by Payan (1978) the use of high-pass filtering enhances the effects of radial distance, and in effect, for the same detection surface area, enhances the contributions from NFs and increases the chance of detecting significant MFPs from NFs. This is essentially the basis of single-fiber EMG whether using a traditional single-fiber or concentric needle electrode (Sanders and Stålberg, 1996; Stålberg, 2012). Because of the enhancement of NF contributions relative to distant fiber contributions, a suitably high-pass filtered concentric or monopolar needle detected MUP is called a NF MUP (NFMUP).

Near fiber electromyography (NFEMG) is the study of NFMUPs for the assessment of neuromuscular changes via the analysis of features related to axonal sprouting and NMJ formation, NMJ transmission time variability or failure and muscle fiber loss, atrophy or hypertrophy. Several previous studies (Allen et al., 2015; Hourigan et al., 2015; Piasecki et al., 2016a; 2016c; 2021; Power et al., 2016; Gilmore et al., 2017; Estruch and Stashuk, 2019; Estruch et al., 2019; Kirk et al., 2019) have used NFEMG features to demonstrate the effects of specific diseases or ageing on individual MUs. In this paper, NFEMG concepts and methods are described, and NFEMG features used to investigate neuromuscular alterations, including a new measure of NF jitter, NFMUP segment jitter, are defined. Specifically, methods for MUP train extraction, MUP high-pass filtering and NFMUP contamination reduction and feature calculation are outlined. MUPs are extracted from simulated EMG signals to explicitly describe and evaluate a range of NFEMG methods and examples of MUP trains recorded from human muscles are presented to demonstrate and explain how NFEMG methods can provide clinically useful information.

2. Methods

2.1. Simulated motor unit potential data

Fig. 1 depicts the effects of fibre diameter variability, NMJ axial location variability (i.e. end plate scatter) and MU remodelling via reinnervation, on MUP shapes. To separately evaluate the effects on MUP and NFMUP template feature values of each of these factors and single fibre jitter on MUP/NFMUP shape instability feature values, specific muscle/EMG detection scenarios were modelled. A commercially available application (EMG Simulator, V3.6, Karlsson, Stalberg) was used to simulate sets of concentric-needle detected EMG signals generated by MUs for which the numbers of fibers, their sizes, and radial and NMJ axial locations relative to the electrode detection surface are known (Stålberg and Karlsson, 2001). A muscle comprised of four MUs was modelled. For each MU, the number of fibers, their fiber diameter and NMJ axial location distributions and jitter, as well as the expected diameter of the MU territory was selected. Firing pattern characteristics of each MU were also selected. Except for specific changes related to the scenarios described below, all muscles were simulated with default properties and signals were simulated using the enlarged uptake area of a concentric needle EMG electrode positioned axially 20 mm from the center of the endplate region, and randomly positioned radially within the territories of the simulated MUs. For each scenario, 10 EMG signals each containing 4 MUP trains were simulated for 10 unique radial needle positions.

2.2. MUP train extraction

To obtain representative as well as MUP/NFMUP shape instability information, a MUP train must be extracted from a recorded EMG signal from which a MUP/NFMUP template is obtained and across which MUP/NFMUP shape instability can be measured. MUP trains can be extracted using level or window triggering or pattern recognition algorithms. In this work, MUP trains were extracted and analyzed using the algorithms contained in DQEMG (Stashuk, 1999a), modified to specifically account for MUP/NFMUP shape instability within a MUP train, via the following steps: 1) MUP detection, 2) initial MUP clustering, 3) supervised MUP classification, 4) MUP train splitting and merging, 5) extracted MUP train characterization. Fig. 2A shows a MUP raster plot (subsequent MUPs displayed consecutively) of a portion of an extracted MUP train. Fig. 2B shows the MUP shimmer plot (subsequent MUPs overlaid) of the MUP train.

2.3. Choice of high-pass filter

To increase the effects of the radial distances to muscle fibers on detected MUPs and thus enhance contributions of near fibers to detected MUPs, the detected EMG signals are high-pass filtered. For conventional single fiber EMG analysis signals are usually filtered using a Butterworth high-pass filter with a 500 or 1000 Hz cut-off frequency. However, (Stashuk, 1999b), has demonstrated how the use of low-pass-double-differentiation filters (Usui and Amidror, 1982; McGill et al., 1985) can produce waveforms in which it is easier to detect single muscle fibre contributions (i.e. MFPs). As such, a NFMUP is obtained by estimating the slopes of the slopes of a MUP waveform, which involves dividing by the square of the sampling rate. NFMUPs are therefore expressed in units of kV/s^2 and NFMUP peaks are associated with points of abrupt MUP amplitude changes and MFP contributions. Fig. 2A shows a MUP train with Fig. 2D and 2E showing the corresponding NFMUP raster and shimmer plots, respectively.

2.4. Definition of MUP and NFMUP template features

Fig. 2C shows the MUP template for the MUP train partially shown in Fig. 2A.

MUP Area - integral of the absolute value of the MUP values between the onset and end markers, times the sampling time interval, in μVms.

MUP Duration - duration between the onset and end markers, in ms.

Turns – number of significant slope reversals within the MUP duration (height > 20 μv)

Fig. 2F shows the corresponding NFMUP template for the NFMUP train partially shown in Fig. 2D, the MUP template is also shown in grey.

NFMUP Area - integral of the absolute value of the NFMUP values between the onset and end markers, times the sampling time interval, in V/s.

NFMUP Duration – duration between the onset and end markers of the NFMUP, in ms.

NF Count – number of fiber contributions detected within the NFMUP duration (i.e. significant positive peaks (height > 5*NF baseline RMS) with similar rising and falling slopes)

NFMUP Dispersion – time between the first and last detected fiber contribution, in ms

2.5. Definition of MUP train features

One objective of analyzing the MUPs comprising a MUP train is to characterize the discharge pattern of the associated motor neuron using the occurrence or detection times of the composite MUPs. An additional objective is to assess jitter. The focus of single fiber EMG is to measure single fibre or fibre pair jitter. During stimulated measurements, the responses of a single fibre to a set of

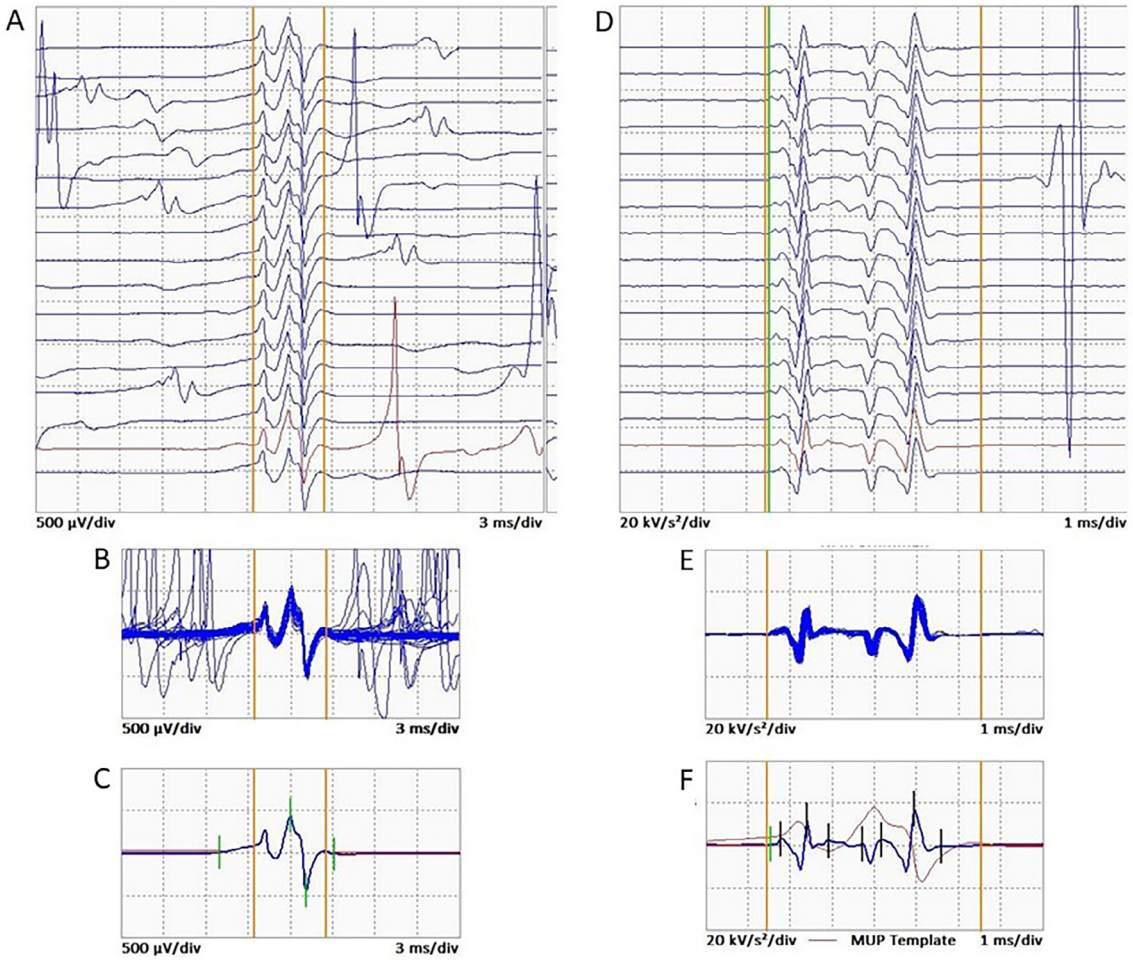

Fig. 2. Partial motor unit potential train raster plot (A), MUP shimmer plot (B), MUP template (C), partial near fibre motor unit potential (NFMUP) train raster plot (D), NFMUP shimmer plot (E), NFMUP template with MUP template shown in grey (F). µV, microvolt; div, division; ms, millisecond; kV/s^2, kilovolt per second squared; MUP, motor unit potential.

stimuli are recorded. During voluntary activation measurements, a set of fiber pair contributions are detected in successive MUPs across a MUP train. In each case, the variance of their inter potential intervals (IPIs) is used to characterize the jitter of the single fibre or fiber pair, respectively. To obtain a feature related to the jitter of a larger number of MU fibres, statistics related to MUP shape instability across a MUP train, such as jiggle, have been developed (Stålberg and Sonoo, 1994). In this work, MUP and NFMUP jiggle have been measured using the MUPs and NFMUPs of MUP/NFMUP trains, respectively.

Jiggle values, which are normalized means of median consecutive amplitude differences, and those of other similar global-MUP-shape based statistics (Stålberg and Sonoo, 1994), indirectly represent the jitter of a larger number of MU fibres than do single fibre or fiber pair jitter measurements. They are dependent on amplitude differences and therefore on the relative sizes/amplitudes of MUP segments, not purely on their temporal variability, and they have normalized units. A new statistic to more directly represent the jitter of near fibres, NFMUP segment jitter, is introduced in this work. Like jiggle, NFMUP segment jitter represents a larger number of MU fibres than do single fibre or fiber pair jitter measurements. However, unlike jiggle, NFMUP segment jitter is independent of the relative sizes/amplitudes of the MUP segments, and instead dependent on their temporal variability and therefore measured in µs. Furthermore, NFMUP segment jitter measurements can be obtained without the need to isolate sets of single fibre or fibre pair contributions and instead provide weighted average measures of the jitter associated with the near fibres significantly contributing to the NFMUPs analyzed.

To accurately assess jitter using extracted MUP trains, the MUPs of each MUP train must first be aligned to each other. In this work, MUPs within a train are aligned during the process of MUP train extraction using methods similar to the correlation maximization method of Campos et al (2000). The method for calculating NFMUP segment jitter is described in Appendix A.

2.6. Definition and selection of isolated MUPs/NFMUPs

To accurately assess jitter using detected MUPs/NFMUPs it is also essential that the MUPs/NFMUPs used represent the activation of a single MU and are not contaminated by the activity of other MUs. Such MUPs/NFMUPs, can be characterized as isolated MUPs/NFMUPs. To select isolated MUPs/NFMUPs within a MUP/NFMUP train, NFMUPs contaminated with contributions of other MUs need to be excluded. MUP/NFMUP contamination will cause a segment of a MUP/NFMUP to have significantly different values than corresponding segments of previous and subsequent MUPs/NFMUPs. Detecting these significant differences must take into account the inherent NFMUP shape instability across a train as well as any trend in NFMUP shape across the train due to needle move-

ment. MUP/NFMUP instability features are calculated over the NFMUP template duration. Therefore, an isolated NFMUP only needs to be contamination free across the NFMUP duration interval. The method for selecting isolated NFMUPs is described in Appendix B.

2.7. Human motor unit potential data

To demonstrate and explain the clinical utility of NFEMG methods three sets of example human MUP data, corresponding to a control, neurogenic and myopathic subject, were selected for NFEMG analysis. Data for all three cases were selected through retrospective review with the approval of the local ethics committee (Biomedical Research Institute, Jiménez Díaz Foundation University Hospital; code EO181-20_FJD). Diagnoses were those made by the examining neurophysiologist (OGC) at the time of the study, based on the results of the clinical and neurophysiological examination. EMG signals were acquired during a sustained mild effort protocol of 10 s duration as part of the routine neurophysiological examination. Intramuscular signals were detected with a standard concentric needle electrode (38 × 0.45 mm (1.5″ x 26G) Neuroline Concentric; Ambu®, Denmark). EMG signals were bandpass filtered (20 Hz – 10 kHz) and stored (24,000 samples/s) using a KeyPoint. Net 3.22® device (Alpine Biomed, USA). NFEMG feature values were generated using DQEMG.

2.8. Statistical analysis

All statistical analysis was completed using STATA (v.15). All feature values within each scenario were assessed across levels of severity (i.e. increasing fiber diameter variability) using multilevel mixed effects linear regression models, with each needle position a fixed factor. Beta (β) coefficients and 95% confidence intervals are reported. Significance was accepted at $p < 0.05$.

3. Results

3.1. Simulated MUP data

3.1.1. Increasing fiber diameter variability

Four sets of 40 MUP trains were extracted from simulated EMG signals based on muscles modeled to have MUs having default mean fiber diameters (50 μm) with diameter standard deviations of 1, 5, 10 and 15 μm. Increased MFP temporal dispersion associated with increased fiber diameter variability decreased MUP area (Fig. 3A) and increased MUP duration (Fig. 3C), but did not affect NFMUP area (Fig. 3B). The number of MUP turns and the NF count increased with the increased MFP temporal dispersion associated with increased fiber diameter variability (Fig. 3D and 3F). Increases in modelled MFP temporal dispersion were clearly and consistently reflected in NFMUP duration and dispersion (Fig. 3E and 3G). MUP and NFMUP jiggle values, and NFMUP segment jitter values all increased across increases in fiber diameter variability. Even though the modelled jitter was constant, across the increasing levels of modelled fiber diameter variability, increased average MFP dispersion caused increased MUP and NFMUP shape instability. However, more consistent increases in MUP versus NFMUP jiggle, evidenced by the larger MUP jiggle relative β coefficient (β/CI), were measured. The temporally-based NFMUP segment jitter values show moderate increases as indicated by the small relative β value.

3.1.2. Increasing end plate scatter (NMJ axial location variability)

Neuromuscular disorders can cause within MUs axial as well as fascicular bound distal axonal sprouting, conduction slowing along small unmyelinated axonal branches, and NMJ transmission delays (Daube, 2000). All of these result in increased dispersion among the MFPs contributing to a MUP generated by a MU. To simulate each of these factors is impractical. However, their combined effects can be studied by varying the amount of NMJ axial location variability (i.e. end plate scatter) modeled. Therefore, five sets of 40 MUP trains were extracted from simulated EMG signals based on muscles modeled to have MUs having default mean fiber diameters (50 μm) and diameter standard deviations (5 μm), and mean axial endplate locations of 0 mm with endplate location standard deviations of 1, 2, 5, 7, and 10 mm. As with increasing fiber diameter variability, increased MFP temporal dispersion associated with increased end plate scatter clearly decreased MUP area (Fig. 4A) and increased MUP duration (Fig. 4C), but only moderately increased NFMUP area (Fig. 4B). The number of MUP turns and NF count values increased with greater endplate scatter (Fig. 4D and 4F). Increases in MFP temporal dispersion are clearly and consistently reflected in NFMUP duration and NFMUP dispersion, with changes greater than for the study of increased fiber diameter variability (Fig. 4E and 4G). Even though the modelled jitter was constant across the increasing levels of modelled end plate scatter, increased average MFP dispersion led to increased MUP and NFMUP shape instability. However, more consistent increases in MUP versus NFMUP jiggle, evidenced by the larger MUP jiggle relative β coefficient (β/CI), were apparent. The temporally-based NFMUP segment jitter values show clear increases as indicated by the large relative β value.

3.1.3. MU diminution and expansion

To consider a simple model of partial/distal denervation and reinnervation with fiber atrophy and hypertrophy, nine sets of 40 MUP trains related to varying degrees of involvement were extracted from simulated EMG signals based on muscles modeled to have MUs with characteristic as outlined in Table 1. Of the MUs modelled for each muscle, 1 is 'heathy', 4 have 'denervated' and 4 have 'compensated/reinnervated' characteristics. Where fiber number is increased, so is fiber diameter variability and endplate scatter.

Fig. 5A shows MUP area decreasing with denervation due to decreasing fiber number and remaining unchanged with reinnervation relative to the 'healthy' model. Only at the highest level of involvement simulated do reinnervated MUs have increased MUP area relative to denervated MUs. MUP duration clearly decreases for denervated and increases for reinnervated MUs (Fig. 5C). NFMUP area, shown in Fig. 5B, did not change with denervation. With reinnervation, NFMUP area was increased with respect to the default and denervated models, but with increased variability no trend with reinnervation was evident. Complexity, as assessed by the number of turns and NF count, did not differ with increased levels of denervation, but did differ with increasing reinnervation, likely as a result of increasing fiber diameter variability and end plate scatter (Fig. 5D and 5F).

With progressive denervation there were no changes in NFMUP duration or NFMUP dispersion. However, both features had increased values with increased reinnervation, again as a result of increased fiber diameter variability and end plate scatter (Fig. 5E and 5G). Similarly, there were no trends in MUP or NFMUP jiggle and segment jitter with increased denervation. With reinnervation, there was no difference in NFMUP jiggle but MUP jiggle and NFMUP segment jitter progressively increased (Fig. 5H-J).

3.1.4. Increasing levels of jitter

Six levels of jitter were modelled (20, 40, 60, 80, 100, and 120 μs). For each jitter level, ten EMG signals each containing 4 MUP trains were simulated for 10 unique radial needle positions. Increased simulated jitter resulted in similar MUP area up to the

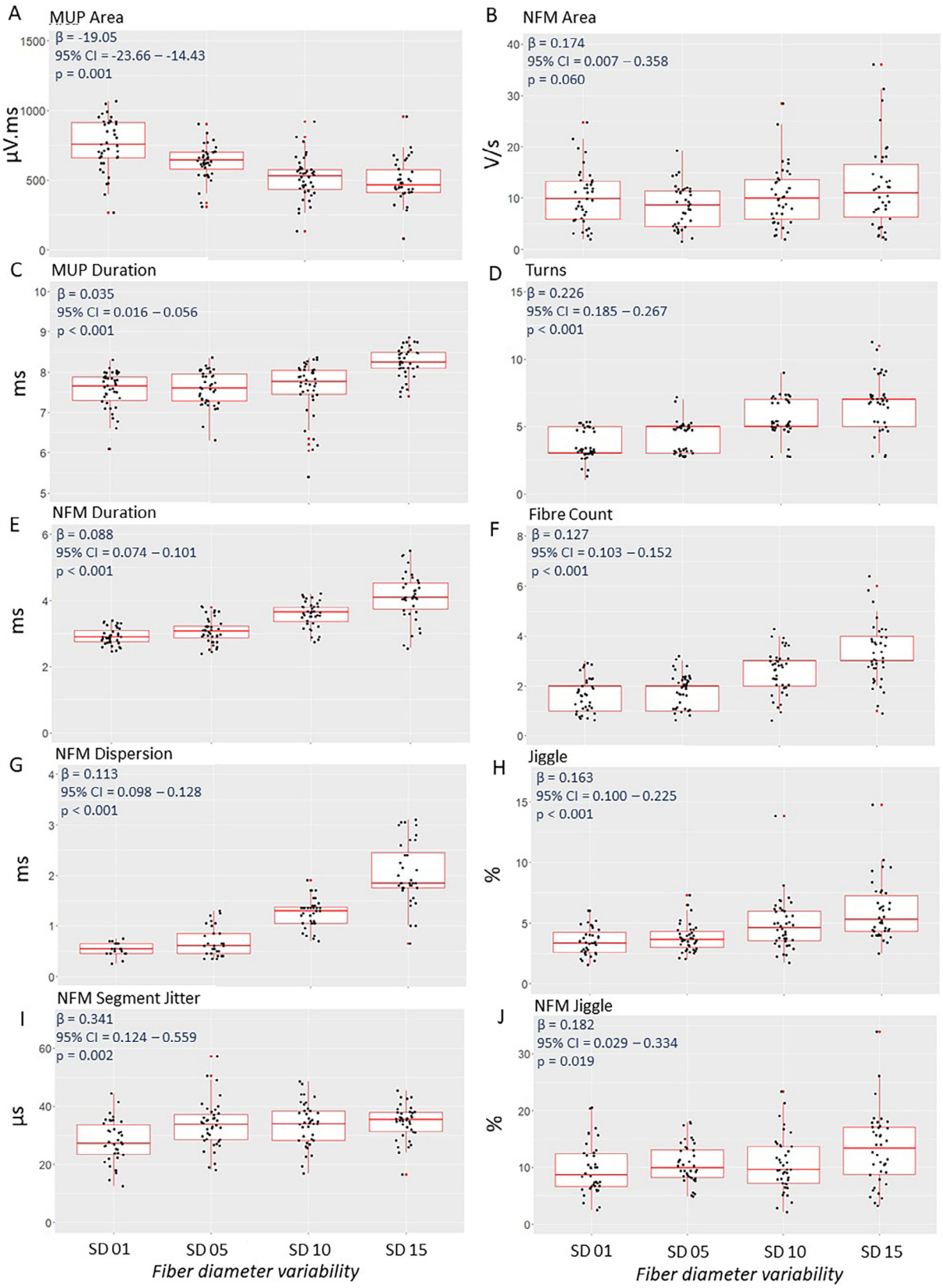

Fig. 3. Motor unit potential and near fiber motor unit potential feature values with increases in fiber diameter variability. Beta coefficients, 95% confidence intervals and p values from multi level mixed effects linear regression shown inset for each feature. MUP, motor unit potential; µV.ms, microvolts millisecond; NFM, near fiber motor unit potential, near fiber motor unit potential; ms, millisecond; µs, microseconds; SD, standard deviation.

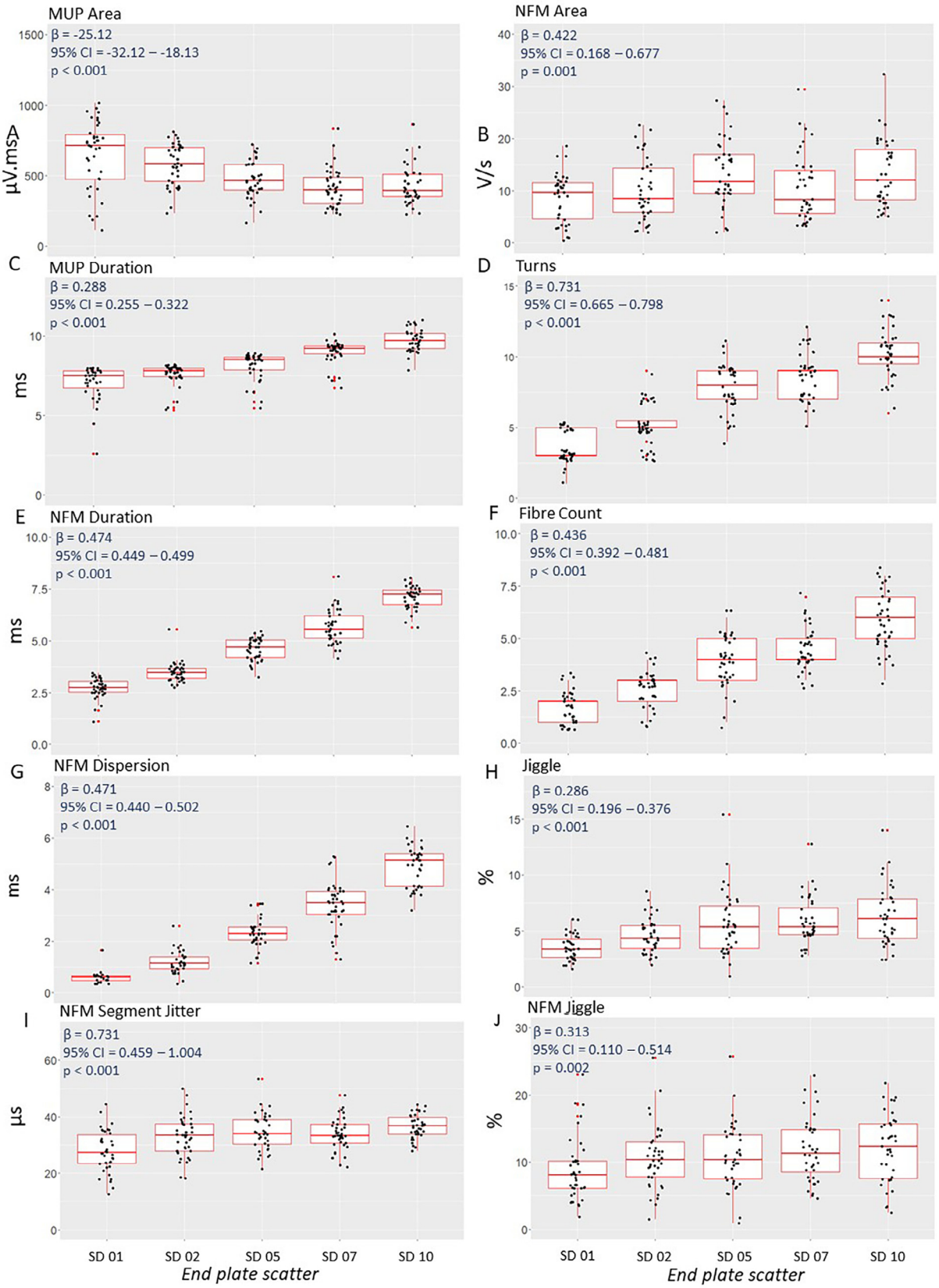

Fig. 4. Motor unit potential and near fiber motor unit potential feature values with increases in end plate scatter. Beta coefficients, 95% confidence intervals and p values from multi level mixed effects linear regression shown inset for each feature. MUP, motor unit potential; μV.ms, microvolts millisecond; NFM, near fiber motor unit potential, near fiber motor unit potential; ms, millisecond; μs, microseconds. SD, standard deviation.

Table 1
Features of remodelled motor units.

	Healthy	Denervated				Reinnervated			
Model		1	2	3	4	1	2	3	4
Fiber number	100	90	80	70	60	110	120	130	140
Fiber Diameter SD	5	5	5	5	5	7	10	13	15
Endplate position SD	1	1	1	1	1	3	5	7	10

Fiber number is the number of motor unit fibers, Fiber Diameter SD is the standard deviation of the motor unit fiber diameters and Endplate position SD is the standard deviation of the axial endplate locations about the mean axial end plate location.

most severe (120 μs jitter), where MUP area was smaller (Fig. 6A). There were no differences in NFMUP area (Fig. 6B), MUP duration (Fig. 6C), MUP turns (Fig. 6D), NFMUP duration (Fig. 6E), NF count (Fig. 6F), or NF dispersion (Fig. 6G) across all increases in jitter studied. MUP jiggle, NFMUP jiggle, and NFMUP segment jitter all increased with increasing modelled jitter (Fig. 6H-J). The temporally-based NFMUP segment jitter values, with units in μs, had the highest β and relative β values.

3.2. Human MUP data

Figs. 7 to 9 show example MUP data from healthy, enlarging/reinnervating and depleted MUs of a control, neurogenic and myopathic subject, respectively.

Fig. 7 shows a normal MUP template, an NFMUP template with moderate duration and dispersion and stable NFMUP raster and shimmer plots from a healthy gastrocnemius.

Fig. 8 corresponds to a 70 y.o. male presenting with progressive asymmetric weakness, muscle mass loss and spasticity over the last year. Needle EMG revealed extended ongoing denervation (i.e. fibrillation potentials and positive sharp waves), fasciculations and reduced recruitment together with polyphasic unstable and enlarged MUPs in three body segments, meeting the definition of ALS. Fig. 8 shows a variety of MUP/NFMUP and NFMUP stability characteristics. In Fig. 8A, two normal shaped and sized MUP templates along with NFMUP templates with increased dispersion and moderately unstable NFMUP shimmer plots are shown. In Fig. 8B, two normal sized MUP templates with increased shape complexity as well as NFMUP templates with increased duration, dispersion and increasingly unstable NFMUP shimmer plots are shown. Fig. 8C displays two enlarged MUP templates associated with NFMUP templates with increased duration and dispersion, and only moderately unstable NFMUP shimmer plots as well as a small MUP template associated with a NFMUP template with increased duration and dispersion and a stable NFMUP shimmer plot.

Fig. 9 corresponds to a middle-aged woman diagnosed with dermatopolymyositis in childhood (IDC10-M33.02) currently on immunosuppressant at low doses for intercurrent arthritis (Azathioprine). She presented with subjective worsening of longstanding symmetric residual weakness in proximal muscles during both moderate and sustained efforts, and was referred to check for a suspected new episode of myositis. Needle EMG did not show evidence of active myositis and routine nerve conduction studies were anodyne. Fig. 9 shows small size MUP templates, complex in shape (increased number of turns) and NFMUP templates with increased NF counts and dispersions, but NF durations in the upper limit of normality and stable NFMUP shimmer plots.

4. Discussion

4.1. Introduction

MUPs are comprised of the summation of MFPs generated by propagating MFAPs. As depicted in Fig. 1, increases in fiber diameter variability (Fig. 1B) and/or endplate scatter (Fig. 1C) increase the spatial dispersion of propagating MFAPs and the corresponding temporal dispersion in expected MFAP arrival times (i.e. the times at which the MFAPs are expected to pass closest to the center of the electrode's active detection surface and consequently the time of the peak values of the corresponding MFPs) which in turn increases MFP temporal dispersion and the number of individual contributing MFPs that can be detected. With increased fibre jitter there is increased MFP jitter as depicted in Fig. 1D. As such, to be able to track MFP contributions to MUPs provides access to useful MU morphological and electrophysiological information. However, because of enlarged uptake areas, it is difficult to detect MFP contributions and their jitter in concentric and monopolar needle MUPs recorded using standard filter settings. Standard high pass filtering can be used to better reveal contributions from individual MFPs but ringing artifacts can confound interpretation. Therefore, using low-pass double-differentiation filtering to reduce artifacts and specific NFMUP features, NFEMG can focus on contributions to recorded potentials from MU muscle fibers near the active detection surface of a needle electrode. Thus NFMUP measurements of the number, temporal dispersion and jitter of contributing MFPs are dependent on local MU morphology and electrophysiology and as such can infer subtle MU changes with ageing and/or disease.

4.2. Simulated MUP data

Increasing fiber diameter variability and end plate scatter, as depicted in Fig. 1B and 1C, respectively, are early effects of neuromuscular disorders and ageing and precursors to changes in MU size and fiber grouping. The ability to detect these initial MU changes potentially allows early more sensitive detection of MU abnormalities. As such, increased values of NF count or NFMUP dispersion, duration and segment jitter can be used clinically to augment the diagnosis and tracking of neuromuscular disorders.

When progressively increasing amounts of fiber diameter variability were modelled, MUP area decreased (MUP amplitude (V_{pp}) also follows the same pattern, values not shown), as a consequence of more destructive MFP superpositions causing phase cancelation, even though the number of contributing muscle fibers remains constant. Notably, these effects would likely be reduced with a smaller axial distance separating the electrode and endplate region. MUP duration, in contrast, increased with increasing fiber diameter variability (Fig. 3C) which can also be a consequence of increased MFP dispersion associated with increasing fiber diameter variability, ultimately increasing the time interval between MUP onset and end positions. These results are consistent with those of Stålberg and Karlsson (2001) who reported both MUP V_{pp} and area decreases for simulated data with increases in MFP dispersion. NFMUP area was not affected by increased fiber diameter variability (Fig. 3B) which can be related to the relatively smaller number of MFPs that make significant contributions to NFMUPs. Turns and NF count both increased with fiber diameter variability (Fig. 3 D, F) without increases in numbers of MU fibers or MU fiber density and specifically due to increases in MFP dispersion allowing increased numbers of MFP contributions to be detected. NFMUP duration

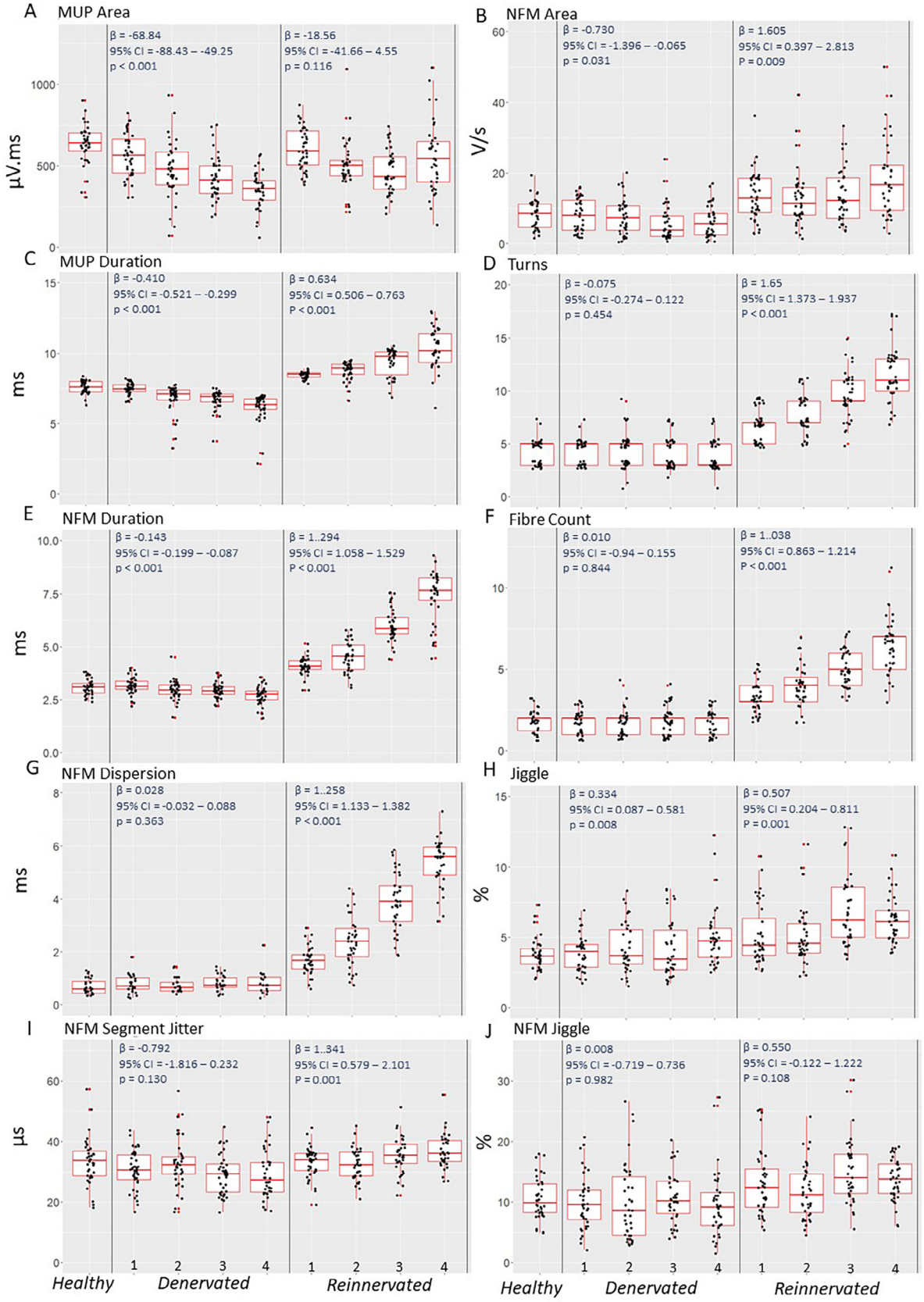

Fig. 5. Motor unit potential and near fiber motor unit potential feature values with decreases or increases in the numbers of MU fibers. For increases in the numbers of MU fibers, fiber diameter variability and end plate scatter are also increased (See Table 1 for details). Beta coefficients, 95% confidence intervals and p values from multi level mixed effects linear regression shown inset for each feature. MUP, motor unit potential; µV.ms, microvolts millisecond; NFM, near fiber motor unit potential, near fiber motor unit potential; ms, millisecond; µs, microseconds.

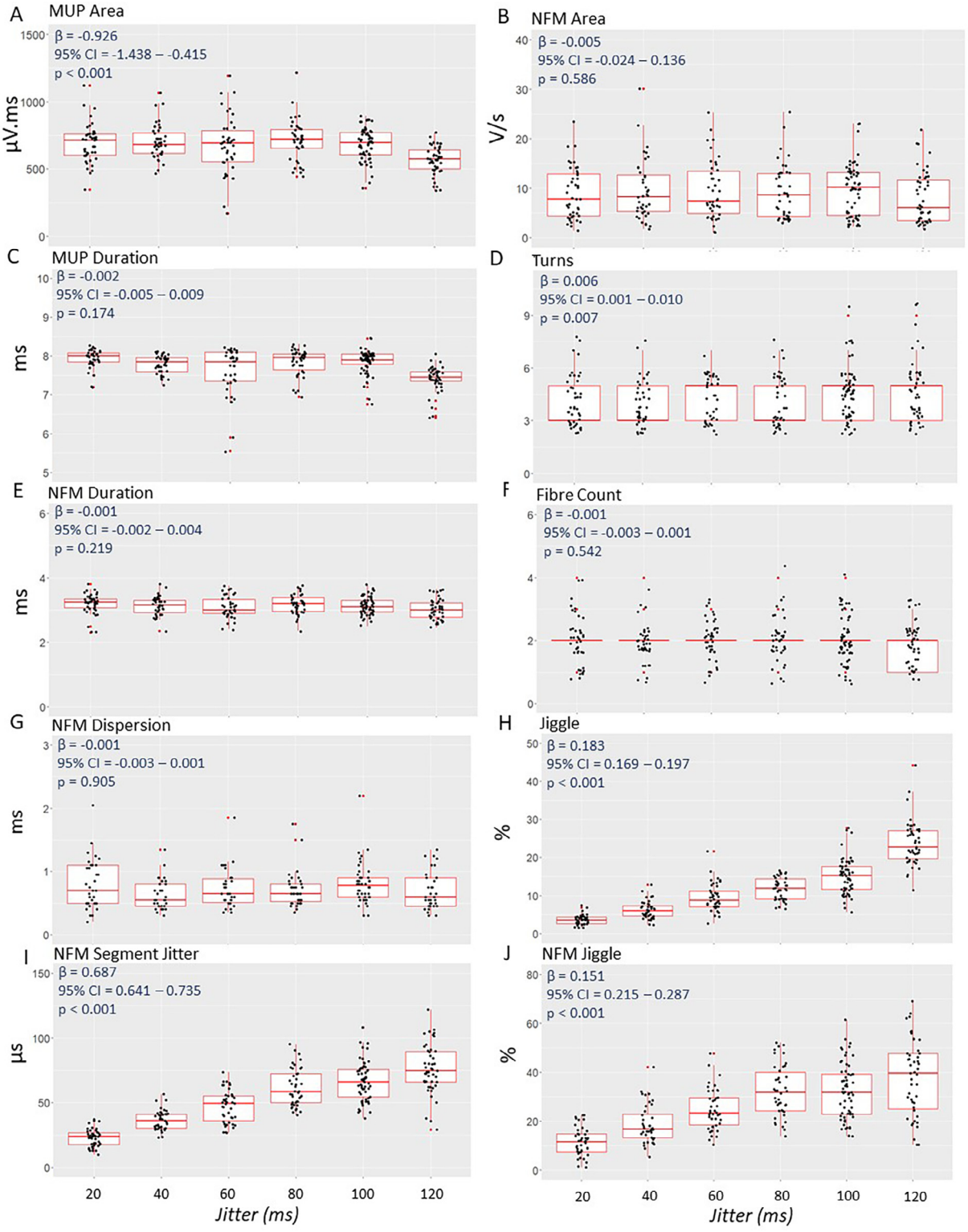

Fig. 6. Motor unit potential and near fiber motor unit potential feature values with increased jitter. Beta coefficients, 95% confidence intervals and p values from multi level mixed effects linear regression shown inset for each feature. μV.ms, microvolts millisecond; NFMUP, near fiber motor unit potential; ms, millisecond; μs, microseconds.

and dispersion both increased with increases in fiber diameter variability (Fig. 3 E,G). Each of these temporal features are directly related to MFP dispersion and clearly reflect increases in MFP dispersion caused by increases in the range of muscle fibre conduction velocities associated with increases in fiber diameter variability. MUP jiggle, NFMUP jiggle and segment jitter across MUP/NFMUP trains all had similar modest increases with increased MFP dispersion associated with increased fiber diameter variability, explained by MFP contributions and their associated jitter becoming easier to observe.

Increased endplate scatter produced similar, yet slightly greater outcomes to those from increased fiber diameter variability, likely

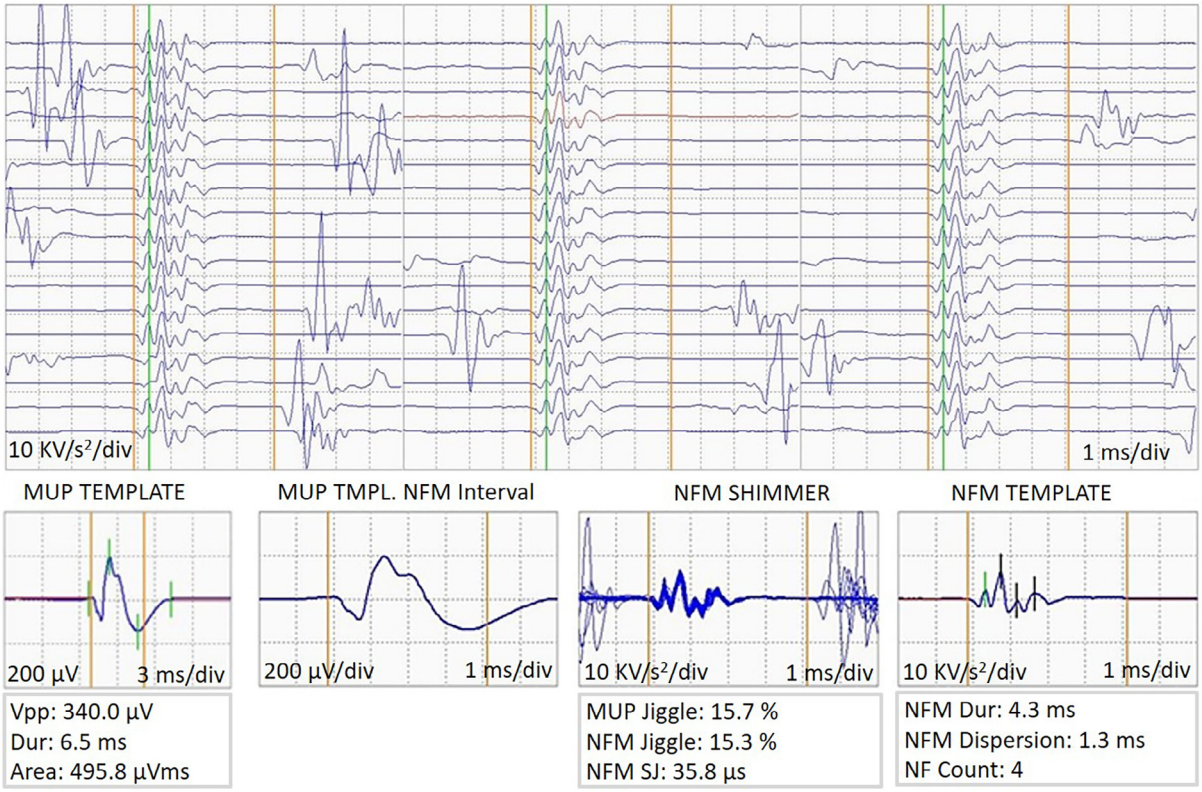

Fig. 7. Data from a healty MU in a healty muscle (gastrocnemius) . A raster of 3, 12 ms sweep, columns of isolated NFMUPs, an 18 and 8 ms sweep MUP template, and an 8 ms sweep NFMUP shimmer and template are shown. The top to bottom vertical lines demarcate the NFMUP duration, in the NFMUP template the elements of the NFMUP count are demarcated by short vertical lines. The interval between the first and last short vertical line is the NFMUP dispersion. Associated MUP and NFMUP template as well as MUP train feature values are shown. The MUP template is of somewhat below average size, the NFMUP template is of average duration and dispersion and the NFMUP raster and shimmer plots are stable. Note that the rasters of isolated NFMUPs as well as the calculated NFMUP segment jitter value indicate healthy NMJ transmission time variability in spite of slight needle movement during signal acquisition. MUP, motor unit potential; NFMUP, near fiber motor unit potential; NFMUP SJ, near fiber motor unit potential segment jitter.

as a result of the former generating greater levels of MFP dispersion compared to the latter. The MUP and NFMUP instability feature values all had similar modest increases, which were, despite the increased amounts of MFP dispersion, similar in extent as with the fiber diameter variability simulations (Fig. 4 H-I).

For MUs with fewer numbers of fibers, MUP area and duration decreased with decreasing numbers of MU fibers (Fig. 5 A, C). The reversal of this pattern could be assumed if all other modelled parameters remained constant. With or without modelled MFP dispersion, MUP V_{pp} and area values were strongly correlated (r = 0.82, data not shown). Without MFP dispersion (denervation), MUP area and MUP duration decreased and reflects the number of MU fibers. However, with MFP dispersion (reinnervation), as depicted in Fig. 1D, MUP area showed little change while MUP duration increased, therefore in this case MUP duration, but not area, may reflect the number of MU fibers (Fig. 5 A, C). NFMUP area is less affected by MFP dispersion than MUP area and duration (Fig. 5B). Therefore, if MFP dispersion is increased, NFMUP area may not be strongly correlated with MUP area or duration but nonetheless can be reflective of the number of MU fibers. NF count is well correlated with number of turns and can equally reflect the MFP dispersion underlying MUP/NFMUP complexity (Fig. 5F). Note, NF count is not directly related to fiber density measurements obtained using a single fiber EMG electrode (Stalberg and Thiele, 1975) because to obtain the latter measurements, the needle is positioned to obtain minimal MUP rise times from a single MU, whereas for the former, the needle is positioned to obtain suitably sharp MUPs across the interference pattern. The constant NFMUP duration and dispersion values across the different levels of denervation combined with their increasing values across the different levels of re-innervation (Fig. 5E, G) highlight their correlation with changing fibre diameter variability and/or endplate scatter and potential ability to detect motor unit morphological changes.

Increased simulated jitter resulted in similar MUP area up to the most severe jitter value simulated (120 µs), where MUP area was smaller (Fig. 6A). There were no differences in NFMUP area (Fig. 6B), MUP duration (Fig. 6C), MUP turns (Fig. 6D), NFMUP duration (Fig. 6E), NF count (Fig. 6F), or NF dispersion (Fig. 5G) across all increases in simulated jitter. MUP jiggle, NFMUP jiggle, and NFMUP segment jitter all increased with increasing modelled jitter (Fig. 6-H-J). The temporally-based NFMUP segment jitter values, with units in µs, had the highest β and relative β values.

The decreases in MUP area and duration values with large amounts of jitter (Fig. 6A, C), are likely due to template estimation errors across the sets of unstable MUPs. The strong correlations between modelled jitter and MUP jiggle and NFMUP jiggle and segment jitter values (Fig. 6H-J) demonstrate a clear relationship that can be clinically utilized. Unlike conventional single fibre or fiber pair jitter, measured using a single-fiber or concentric needle electrode to detect a set of MFP contributions from a single fibre or an isolated pair of fibers (Sanders and Stålberg, 1996; Stålberg and Sanders, 2009), MUP and NFMUP jiggle and segment jitter represent an amount of temporal variability measured across all of the MFPs significantly contributing to the MUPs/NFMUPs of a MUP/NFMUP train and do not require the existence of individual or distinct pairs of MFP contributions. Jiggle expresses MFP temporal

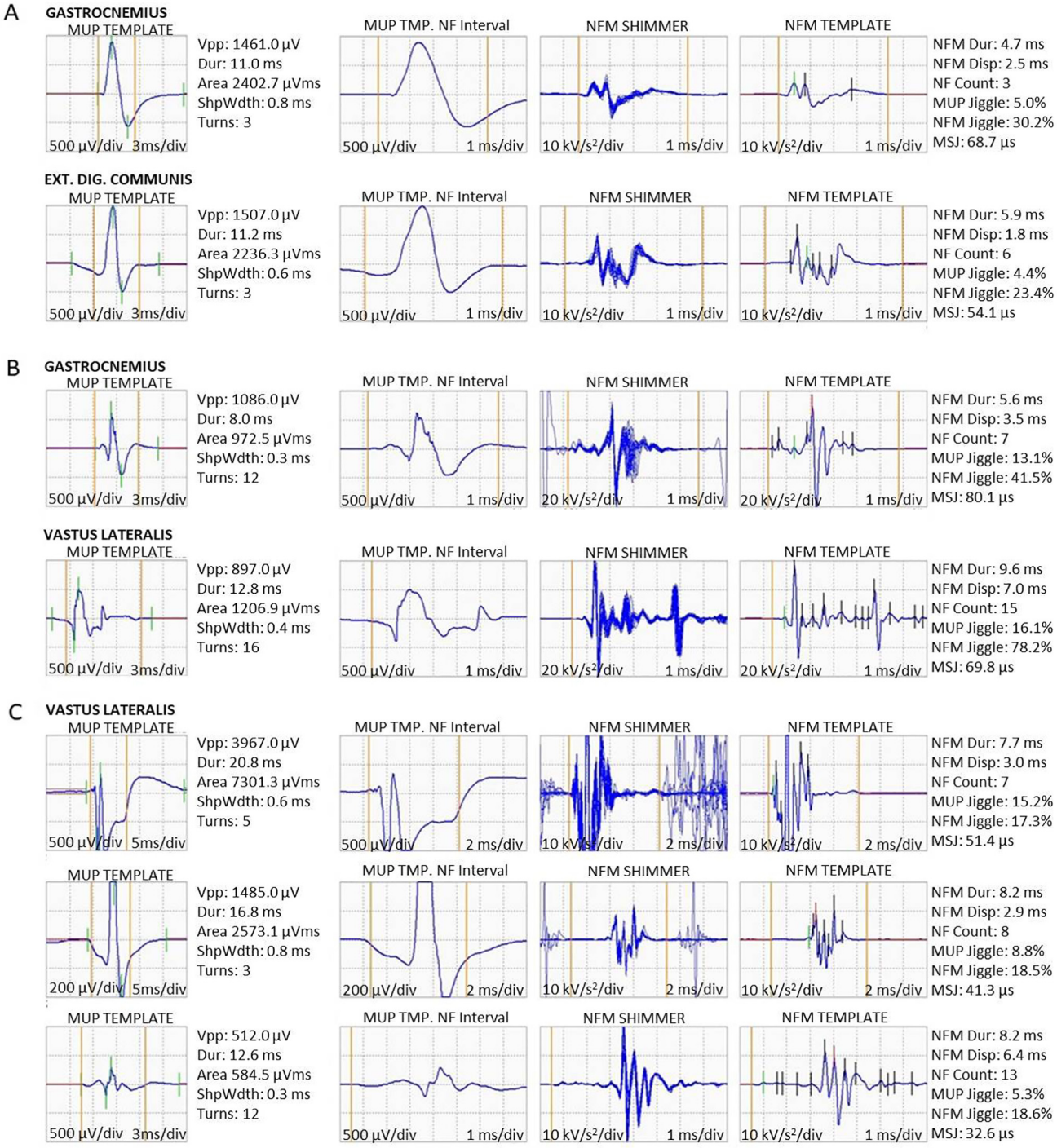

Fig. 8. Different stages of reinnervation are depicted across 8A-C. In 8A emerging reinnervation is manifested as increased NFMUP shape instability and a mild rise in NFMUP duration and dispersion. In 8B reinnervation is prominent, showing a complex shaped MUP with increased NFMUP feature values. In 8C three stable MUPs are depicted. From top to bottom, MUP size wanes yet with increased temporal dispersion (high NFMUP duration and dispersion). It is hypothesised that progression of certain neurogenic disorders can cause partial denervation (see text). Note that the bottom MUP in 8C is mainly a downward positive potential (i.e. a cannula potential), yet NFEMG is able to extract valuable information from it. From left to right: MUP template, MUP template NFMUP interval, NFMUP shimmer and NFMUP template are displayed. The top to bottom vertical lines demarcate the NFMUP duration. MUP, motor unit potential; NFMUP, near fiber motor unit potential; NFMUP SJ, near fiber motor unit potential segment jitter.

variability (primarily due to NMJ transmission time variability) by measuring MUP/NFMUP instability along the amplitude axis. Jiggle, measured using sums of median consecutive absolute amplitude differences, which reduce the effects of small needle movements and contamination from other MUs, and the ratio to template area, which reduces the effects of needle focusing/positioning, was determined the best of several instability features considered by Stålberg and Sonoo, (1994). Nonetheless, in real signals, MUP jiggle values are more contaminated by contributions from other MUs (Campos et al., 2000) than are NFMUP jiggle or segment jitter values. Algorithms used in this work to extract MUP trains and to select isolated MUPs/NFMUPs are specifically

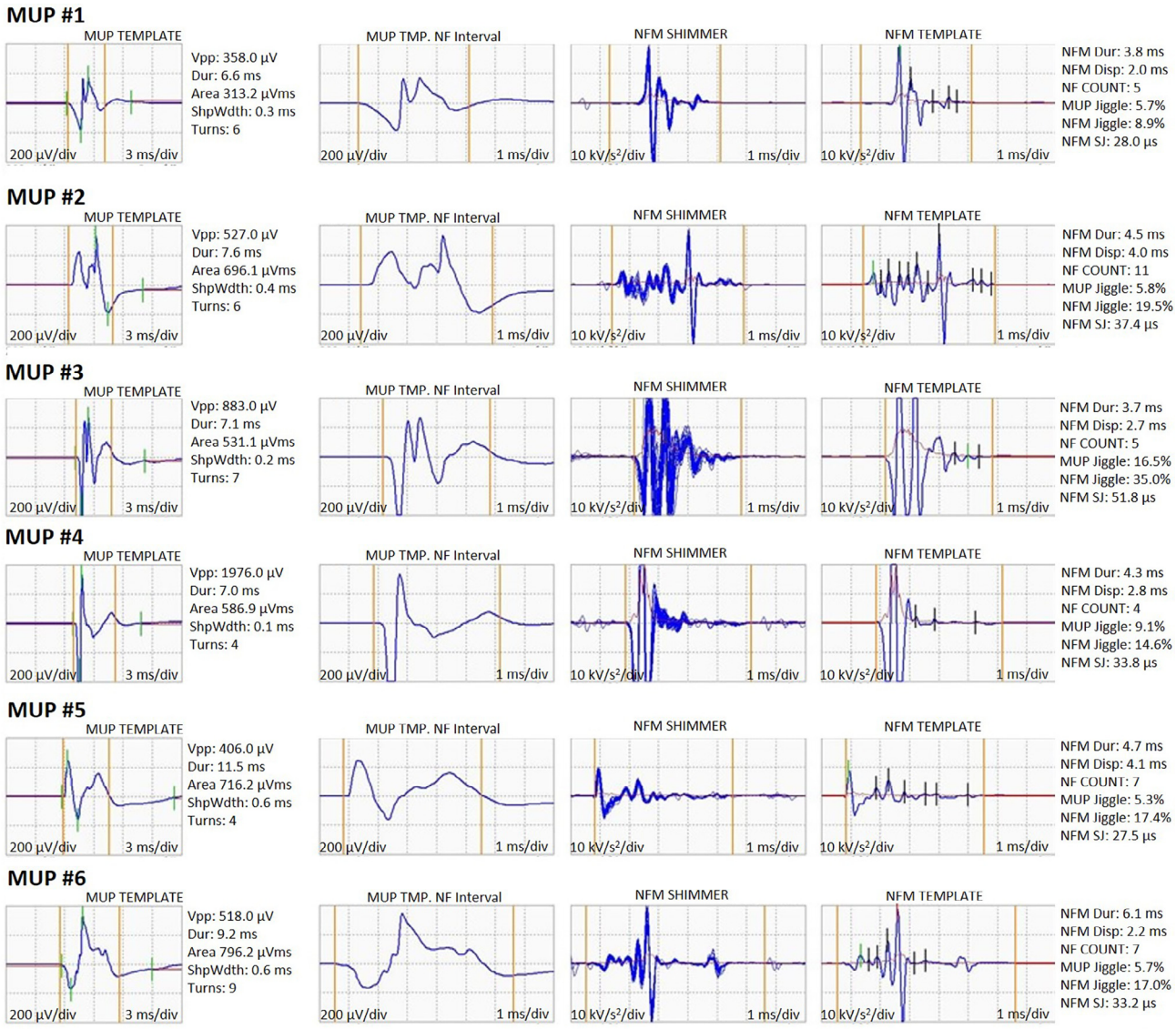

Fig. 9. Example of a mild myopathic deltoid showing MUPs of partially depleted MUs recorded during a low level isometric contraction. Each row corresponds to individual MUs from the same contraction. From left to right: MUP template, MUP template NFMUP interval, NFMUP shimmer and NFMUP template are displayed. The top to bottom vertical lines demarcate the NFMUP duration. MUP, motor unit potential; NFMUP, near fiber motor unit potential; NFMUP SJ, near fiber motor unit potential segment jitter.

designed to account for MUP/NFMUP instability, to minimize the effects of needle positioning/focusing and to effectively align MUPs/NFMUPs for instability assessment to reduce contamination and other sources of instability measurement error described in earlier works (Campos et al., 2000; Stålberg and Sonoo, 1994).

With jitter held at a constant "reference" value (25 µs), MUP and NFMUP jiggle and segment jitter increased with MFP temporal dispersion as the effects of more individual MFP components could be determined (Fig. 3 H-J and Fig. 4 H-J). However, the increased values do not exceed "reference" values (<50%, < 50 µs). Stålberg and Sonoo (1994) discussed how MUP polyphasia, caused by increased MFP temporal dispersion exposes inherent/true instability which can be masked with decreased MFP temporal dispersion where jittering MFPs are simply consistently superimposed such that the apparent/measurable jitter/temporal instability is reduced. In other words, increases in instability feature values can be solely caused by increases in MFP temporal dispersion as the inherent/electrophysiological temporal variability can be more accurately measured. This in turn suggests that increased polyphasia without increased jiggle can indicate chronic myopathic fiber diameter variability increases (Stålberg and Sonoo, 1994). MUP jiggle was more severely influenced by mean MFP temporal dispersion than were NFMUP jiggle and segment jitter, and NFMUP segment jitter was affected more by mean MFP temporal dispersion than was NFMUP jiggle. Due to the larger MUs simulated, 100^{+} here versus their 10 fibers, the drop in MUP jiggle versus MU size reported by Stålberg and Sonoo was not apparent in this data for either MUP and NFMUP jiggle or segment jitter (Fig. 5 H-J). Even though for small amounts of jitter (20 µs), its mean values were relatively high and for high amounts of jitter (100 and 120 µs) its mean values were relatively low, the temporally based NFMUP segment jitter feature had the strongest relationship with increasing jitter. Because increases in NFMUP segment jitter more closely track those of simulated jitter it can be considered more directly related to the electrophysiological temporal variability of MFP contributions to MUPs than are MUP and NFMUP jiggle, and is therefore more sensitive for detecting MU electrophysiological temporal variability.

4.3. Human MUP data

Results from a healthy MU (Fig. 7) show a moderate MUP area (size), with average NFMUP duration and dispersion and stable NFMUP raster and shimmer plots (healthy jitter). The two MUPs with slightly increased, but still within the normal range, area and duration and their corresponding NFMUPs with incipient increases in NF count, duration and dispersion and increased segment jitter, shown in Fig. 8A, reflect MUs with increased jitter at initial/early stages of reinnervation. The two MUPs of average size but increased shape complexity and their corresponding NFMUPs with prominent increases in NF count, duration, dispersion and segment jitter, shown in Fig. 8B, reflect prominently reinnervated MUs with increased jitter. The enlarged, moderately enlarged and reduced size MUP and their corresponding NFMUPs with similar and increased NF count, duration and dispersion and rather stable segment jitter, shown in Fig. 8C, possibly reflect distal axonal damage affecting longstanding enlarged and stable MUs (de Carvalho and Swash, 2016). The NF count and NFMUP duration and dispersion values for these MUs are clearly greater than for the healthy MU, shown in Fig. 7, and greater than for any values obtained from simulations of only increased fiber diameter variability, suggesting some degree of axonal sprouting with conduction slowing in unmyelinated, small diameter axonal branches, and possibly some NMJ transmission delays and increased MU fiber diameter variability consistent with reinnervation of possibly atrophied fibres (Daube 2000).

When considering myopathic depleted MUs, NF count and NFMUP duration and dispersion values for all of the MUs shown in Fig. 9 (6/26 of the total number of MUs sampled) are greater than for healthy MUs and greater than for any values obtained from simulations of only increased fiber diameter variability. This suggests some degree of axonal sprouting with conduction slowing as well as possibly some increased MU fiber diameter variability consistent with fiber atrophy, splitting and/or hypertrophy. Reduced MUP areas and normal durations, together with normal valued NFMUP stability features indicate a steady-state, with no evidence of ongoing reinnervation as a sign of recent myositis. This selected myopathic case, in effect, shows both myopathic and subtle chronic and stable MU remodelling that cannot be detected using classic MUP size features. Also, no reinnervating features were detected, thus allowing a response to the critical question of the referring physician as to whether a recent episode of myositis had taken place. This illustrates the overarching capabilities of NFEMG to profile both complexity and stability features, which help determine the time course of the disease. In this case, the NFEMG data obtained accurately fits the clinical evolution of the case presented (i.e., a chronic muscle disease with very few recognized episodes of myositis since the childhood diagnosis, and being currently in a steady state).

4.4. Practical aspects

The example MUP data was selected retrospectively from studies conducted as part of a routine neurophysiological examination. As such, no special recording electrode or protocol are required to obtain useful NFEMG feature values. For this study MUP trains were extracted using DQEMG. During MUP train extraction DQEMG does not interfere with new data acquisition nor with other applications. DQEMG can operate on-line or off-line, with an average analysis time of 30 s per 10 s of analyzed signal. When on-line, DQEMG allows editing/reviewing processed results while concurrently analyzing other signals in the background. Three of the 14 example MUPs have an initial negative deflection suggesting detection directly over a MU endplate zone and one has an initial positive deflection and a limited negative phase suggesting that it is primarily composed of contributions detected by the cannula (i.e. that it is a cannula potential). MUPs with these characteristics are usually excluded from analysis because with decreased axial recording distance from an endplate zone MUP complexity can be decreased and with increased amounts of cannula contributions MUP size and complexity can be changed such that the MUPs may not accurately reflect the sampled MUs. However, all of the NFMUPs associated with these four MUPs provide useful clinical information with respect to NF count and NFMUP duration, dispersion and segment jitter values. This emphasizes an advantage of using decomposition-based QEMG methods in general, and specifically in conjunction with NFEMG methods, during which needle positioning need not be excessively time consuming, searching for iconic MUPs, but rather simply obtaining a needle position at which suitably sharp MUPs are detected.

While a comprehensive method/protocol for the clinical use of NFEMG features has not been presented, and while clinically, most individual QEMG motor unit feature values are "normal" with the focus being on outlying values, and even though it is not possible, for a given MU, to ascertain if increased NFMUP duration and dispersion are caused by increases in fibre diameter and/or end plater scatter variability, from the simulation and example data presented, it is clear that NFEMG can detect subtle changes in otherwise normal MUPs. Thus, depending on the degree and number of MUPs affected, average and/or outlying NFEMG features can be used to characterize the muscle under study. Moreover, the distribution of feature values across MUs and muscles studied can reveal a tendency toward disease, in addition to a threshold-based classification. Although MUP area has shown high test retest reliability in human muscles (Piasecki et al., 2018), further study will establish additional reference values and clinically effective combinations of MUP and NFEMG features to consider.

5. Conclusion

Standard needle EMG examination can detect denervation, reinnervation, fibre loss, atrophy and hypertrophy, but detecting initial changes and quantifying their extent and progress requires more sophisticated techniques which can also provide a temporal profile of a disease process across longitudinal examinations. The data presented here demonstrate that NFEMG methods can augment a standard needle EMG examination with quantitative MU morphological and electrophysiological information and can be applied to study the neuromuscular effects of specific disease processes and ageing.

Declaration of Competing Interest

The authors declare that they have no known competing financial interests or personal relationships that could have appeared to influence the work reported in this paper.

Acknowledgements

Mathew Piasecki is supported by the Medical Research Council [grant number MR/P021220/1] as part of the MRC-Versus Arthritis Centre for Musculoskeletal Ageing Research awarded to the Universities of Nottingham and Birmingham, and by the NIHR Nottingham Biomedical Research Centre.

Appendix A. Calculation of NFMUP segment jitter (NFMUP_SJ)

NFMUP SJ is calculated across a set of isolated NFMUPs selected from a NFMUP train.

An isolated NFMUP is one that is not significantly contaminated by the activity of other MUs and represents the activity of a single MU (see Appendix B).

Each NFMUP in the selected set is itself a set of consecutive sample values.

Given a set of N, isolated NFMUPs, $NFMUP_i$ represents the i^{th} NFMUP of the set and $NFMUP_{ij}$ represents the jth sample of the ith NFMUP.

Fig. 2D shows a raster plot of a portion of a set of isolated NFMUPs selected from a NFMUP train. $NFMUP_i$ would be the ith waveform of this raster plot.

To calculate NFMUP SJ, each NFMUP in the set is individually segmented and each of its segments is temporally aligned with the preceding and following NFMUP of the set.

A NFMUP segment is a continuous section of a NFMUP over which the absolute change in the NFMUP amplitude is equal to a threshold amount, segmentHeight.

The number of segments in each NFMUP is dependent on the specific characteristics of the NFMUP such that $NFMUP_i$ has S_i segments.

$NFMUP\_Seg_{ij}$ is the j^{th} segment of i^{th} NFMUP.

A given $NFMUP\_Seg_{ij}$ is a set of consecutive samples of $NFMUP_i$

such that if k is the starting index in $NFMUP_i$ of the j^{th} segment and p is the ending index in $NFMUP_i$ of the j^{th} segment, $|NFMUP_{ik} - NFMUP_{ip}|$ = segmentHeight

The segments of a NFMUP are contiguous such that first sample of the next segment is immediately after the last sample of the previous segment.

To represent the total amount of alignment required across all of the NFMUPs in the set a nested set of iteration loops are used. The outer loop iterates across the NFMUPs in the set and the inner loop iterates across the segments discovered in each individual NFMUP.

WeightedShiftSum = 0 (Initialize a sum of weighted temporal alignment shift absolute values)

SumOfWeights = 0 (Initialize a sum of alignment shift similarity/confidence values)

For i = 1 to i = N (Iterate across the N NFMUPs in the selected set)

For j = 1 to j = S_i (For each NFMUP, iterate across the S_i segments created for the i^{th} NFMUP)

If (i < N) (Align $NFMUP\_Seg_{ij}$ with the next NFMUP)

Calculate the optimal temporal shift s_{ij} between $NFMUP\_Seg_{ij}$ and $NFMUP_{i+1}$

by successively shifting $NFMUP\_Seg_{ij}$ relative to $NFMUP_{i+1}$ to maximize their shape similarity w_{ij}

Weight the current temporal shift by the current shape similarity and add its weighted absolute value to the weighted sum (s_{ij} may be positive or negative)

WeightedShiftSum = WeightedShiftSum + $|s_{ij}{}^{*}w_{ij}|$

Sum up the similarity weights used (w_{ij} is always a positive value)

SumOfWeights = SumOfWeights + w_{ij}

If (i > 1) (Align $NFMUP\_Seg_{ij}$ with the previous NFMUP)

Calculate the optimal temporal shift s_{ij} between segment $NFMUP_{ij}$ and $NFMUP_{i-1}$

by successively shifting $NFMUP_{ij}$ relative to $NFMUP_{i-1}$ to maximize their shape similarity w_{ij}

Weight the current alignment shift by the current shape similarity and add its weighted absolute value to the weighted sum

WeightedShiftSum = WeightedShiftSum + $s_{ij}{}^{*}w_{ij}$

Sum up the similarity weights used (w_{ij} is always a positive value)

SumOfWeights = SumOfWeights + w_{ij}

Once all of the segments of all of the N NFMUPs in the set have been considered

calculated the NFMUP SJ as a weighted average.

NFMUP SJ = WeightedShiftSum / SumOfWeights

In this work, the value of segmentHeight was the greater of 0.10% of the NFMUP template peak to peak voltage and 5 times the baseline RMS.

The value of s_{ij} was constrained to be in the range between −200 μs to + 200 μs.

Appendix B. Selecting isolated NFMUPs

An isolated NFMUP is not significantly contaminated by the activity of other MUs and represents the activity of a single MU.

A set of isolated NFMUPs allows estimation of the underlying electrophysiological instability of the NFMUPs generated by a MU.

Given a set of N, NFMUPs in a NFMUP train, $NFMUP_i$ represents the i^{th} NFMUP of the train.

Each NFMUP in a NFMUP train is itself a set of consecutive sample values.

Therefore, $NFMUP_{ij}$ represents the jth sample of the ith NFMUP of the train.

Let NFMUP_t be the NF MUP template used to represent the N, NFMUPs of the MUP train.

The NFMUP_t of the MUP train is divided into S_t segments.

A NFMUP_t segment is continuous section of the NFMUP_t over which the absolute change in amplitude is equal to a threshold amount, segmentHeight.

$NFMUP\_t\_Seg_j$ is the j^{th} segment of the NFMUP_t.

$NFMUP\_t\_Seg_{ij}$ is the j^{th} segment of i^{th} NFMUP_t.

A given $NFMUP\_t\_Seg_{ij}$ is a set of consecutive samples of NFMUP_t

such that if k is the starting index in NFMUP_t of the j^{th} segment and p is the ending index in NFMUP_t of the j^{th} segment, $|NFMUP\_t_k - NFMUP\_t_p|$ = segmentHeight

The segments of a NFMUP_t are contiguous such that first sample of the next segment is immediately after the last sample of the previous segment.

Each of the N NFMUPs in the MUP train are positioned as rows in a two dimensional array with N rows and m columns, where m is the number of samples in NFMUP_t.

Each of the N NFMUPs in the NFMUP train are segmentally aligned with the respective S_t segments of NFMUP_t to produce m columns of N aligned NFMUP values.

Across each of the m aligned NFMUP value columns an average mean absolute consecutive difference (MACD) is calculated, with $MACD_j$ being the value for the j^{th} column.

A NFMUP is considered isolated if across all of its samples, (i = 1 to m), the average absolute deviation of q consecutive samples, centered at the i^{th} sample respectively, from q corresponding samples of the previous isolated NFMUP and from q corresponding samples of the NFMUP template are less than $10{*}MACD_i$, where q corresponds to the number of samples required to span 100 μs.

Having a vector of MACD values allows the level of expected variation (i.e. the amount of acceptable contamination) to be different for each time point across the set of NFMUPs with in the NFMUP train. Therefore, the threshold values used as criteria for significant contamination in the baseline segments of the NFMUP train will be more restrictive (have smaller values) than the threshold values used during the higher energy segments. This in turn, allows the shape variability across the NFMUPs of the NFMUP train

to be accurately measured. The alignment of portions of the NFMUPs with the NFMUP template allow for more accurate estimation of the noise present.

References

Allen MD, Stashuk DW, Kimpinski K, Doherty TJ, Hourigan ML, Rice CL. Increased neuromuscular transmission instability and motor unit remodelling with diabetic neuropathy as assessed using novel near fibre motor unit potential parameters. Clin Neurophysiol 2015. https://doi.org/10.1016/j.clinph.2014.07.018.

Campos C, Malanda A, Gila L, Segura V, Lasanta I, Artieda J. Quantification of jiggle in real electromyographic signals. Muscle Nerve 2000;23:1022–34.

de Carvalho M, Swash M. Lower motor neuron dysfunction in ALS. Clin Neurophysiol 2016;127:2670–81.

Daube JR. Electrodiagnostic studies in amyotrophic lateral sclerosis and other motor neuron disorders. Muscle Nerve 2000;23:1488–502.

Estruch OGC, Cano GD, Stashuk D. P32-S Application of decomposition based quantitative EMG (DQEMG) to focal neuropathies. Clin Neurophysiol 2019;130 e104.

Estruch OGC, Stashuk D. P36-S Validation of near fiber motor unit potential stability and dispersion measures using simulated signals. Clin Neurophysiol 2019;130 e104.

Gilmore KJ, Morat T, Doherty TJ, Rice CL. Motor unit number estimation and neuromuscular fidelity in 3 stages of sarcopenia. Muscle Nerve 2017;55:676–84.

Heckman CJ, Enoka RM. Motor unit. *Compr Physiol* 2012;2:2629–82.

Hourigan ML, McKinnon NB, Johnson M, Rice CL, Stashuk DW, Doherty TJ. Increased motor unit potential shape variability across consecutive motor unit discharges in the tibialis anterior and vastus medialis muscles of healthy older subjects. Clin Neurophysiol 2015;126:2381–9.

Katz B, Miledi R. The measurement of synaptic delay, and the time course of acetylcholine release at the neuromuscular junction. Proc R Soc London Ser B Biol Sci 1965;161:483–95.

Kirk EA, Gilmore KJ, Stashuk DW, Doherty TJ, Rice CL. Human motor unit characteristics of the superior trapezius muscle with age-related comparisons. J Neurophysiol 2019. https://doi.org/10.1152/jn.00138.2019.

McGill KC, Cummins KL, Dorfman LJ. Automatic Decomposition of the Clinical Electromyogram. IEEE Trans Biomed Eng 1985;32:470–7.

Payan J. The blanket principle: A technical note. Muscle Nerve 1978;1:423–6.

Piasecki J, Inns TB, Bass JJ, Scott R, Stashuk DW, Phillips BE, Atherton PJ, Piasecki M. Influence of sex on the age-related adaptations of neuromuscular function and motor unit properties in elite masters athletes. J Physiol 2021;599:193–205.

Piasecki M, Ireland A, Coulson J, Stashuk DW, Hamilton-Wright A, Swiecicka A, Rutter MK, McPhee JS, Jones DA. Motor unit number estimates and neuromuscular transmission in the tibialis anterior of master athletes: evidence that athletic older people are not spared from age-related motor unit remodeling. Physiol Rep 2016. https://doi.org/10.14814/phy2.12987.

Piasecki M, Ireland A, Jones DA, McPhee JS. Age-dependent motor unit remodelling in human limb muscles. Biogerontology 2016b;17:485–96.

Piasecki M, Ireland A, Piasecki J, Stashuk DW, McPhee JS, Jones DA. The reliability of methods to estimate the number and size of human motor units and their use with large limb muscles. Eur J Appl Physiol 2018;118:767–75.

Piasecki M, Ireland A, Stashuk D, Hamilton-Wright A, Jones DA, McPhee JS. Age-related neuromuscular changes affecting human vastus lateralis. J Physiol 2016c;594:4525–36.

Power GA, Allen MD, Gilmore KJ, Stashuk DW, Doherty TJ, Hepple RT, Taivassalo T, Rice CL. Motor unit number and transmission stability in octogenarian world class athletes: Can age-related deficits be outrun?. J Appl Physiol 2016;121:1013–20.

Sanders DB, Stålberg EV. AAEM minimonograph 25: Single-fiber electromyography. Muscle Nerve 1996;19:1069–83.

Siegelbaum S & Koester J (2013). Membrane Potential and the Passive Electrical Properties of the Neuron. In: Kandel EC, Schwartz J (editors). Principles of Neural Science, 5th edn. Available at: https://neurology.mhmedical.com/book.aspx?bookid=1049.

Sonoo M. New attempts to quantify concentric needle electromyography. Muscle Nerve 2002;999:S98–S102.

Stålberg E. Jitter analysis with concentric needle electrodes. Ann N Y Acad Sci 2012;1274:77–85.

Stålberg E, Karlsson L. Simulation of the normal concentric needle electromyogram by using a muscle model. Clin Neurophysiol 2001;112:464–71.

Stalberg E, Thiele B. Motor unit fibre density in the extensor digitorum communis muscle. Single fibre electromyographic study in normal subjects at different ages. J Neurol Neurosurg Psychiatry 1975;38:874–80.

Stålberg EV, Sanders DB. Jitter recordings with concentric needle electrodes. Muscle Nerve 2009;40:331–9.

Stålberg EV, Sonoo M. Assessment of variability in the shape of the motor unit action potential, the "jiggle", at consecutive discharges. Muscle Nerve 1994;17:1135–44.

Stashuk DW. Decomposition and quantitative analysis of clinical electromyographic signals. Med Eng Phys 1999a;21:389–404.

Stashuk DW. Detecting single fiber contributions to motor unit action potentials. Muscle Nerve 1999b;22:218–29.

Usui S, Amidror I. Digital Low-Pass Differentiation for Biological Signal Processing. IEEE Trans Biomed Eng 1982;29:686–93.